Environ Geol (2006) 49: 536–551
DOI 10.1007/s00254-005-0081-4

ORIGINAL ARTICLE

M. Sherif
A. El Mahmoudi
H. Garamoon
A. Kacimov
S. Akram
A. Ebraheem
A. Shetty

Geoelectrical and hydrogeochemical studies for delineating seawater intrusion in the outlet of Wadi Ham, UAE

Received: 18 September 2004
Accepted: 5 August 2005
Published online: 26 November 2005

M. Sherif (✉)
Civil and Environmental Engineering Dept., College of Engineering, UAE University, Al Ain, UAE
E-mail: msherif@uaeu.ac.ae

A. E. Mahmoudi · H. Garamoon
Geology Department, College of Science, UAE University, Al Ain, UAE

A. Kacimov
Department of Soil and Water Sciences, College of Agriculture, SQU, Muscat, Sultanate Oman

Abstract The Quaternary aquifer of Wadi Ham, UAE has been overexploited during the last two decades to meet the increasing water demands. As a result, the dynamic balance between freshwater and seawater has been disturbed and the quality of the groundwater has deteriorated. In this paper, a 2D earth resistivity survey was conducted in Wadi Ham in the area between Fujairah and Kalba to delineate the seawater intrusion. Existing monitoring wells were used to measure the horizontal and vertical variations in water salinity and thus to improve the interpretation of earth resistivity imaging data. Results of vertical electrical soundings and chemical analyses of collected water samples were used to obtain an empirical relationship between the inferred earth resistivity and the amount of total dissolved solids. This relationship was used along with the true resistivity sections resulting from the inversion of 2D resistivity data to identify three zones of water-bearing formation (fresh, brackish, and salt-water zones). Along the four 2D resistivity profiles, the depth to the fresh-brackish interface exceeded 50 m at the western part of the area and was in the order of 10 m or less in the eastern side near the shoreline. Depth to the brackish-saline water interface reached about 70 m in the western side and was in the order of 20 m in the eastern side. The thickness of the fresh water zone decreases considerably in the farming areas toward Kalba and thus the degree of seawater intrusion increases.

Keywords Seawater intrusion · Transition zone · 2D earth resistivity imaging · Wadi Ham · UAE

Introduction

The saturated part of the alluvial gravels in Wadi Ham which is directly recharged from the infiltration of rainwater is considered to be the main source of groundwater in this outlet area of Wadi Ham (Fig. 1). The balance between fresh water body in the aquifer and the saline water body intruding from the Gulf of Oman has been upset due to the excessive pumping to meet the rapid increase of water demands for agriculture purposes during the last two decades. On the other hand, drought conditions prevailed since 1996 and more groundwater was pumped to encounter the lack of surface water. Records indicate that groundwater has reached its lowest ever level in 2004. Many wells have dried up and several farms have been abandoned. This severe decline in the groundwater levels is naturally associated with a significant deterioration in the groundwater quality. The seawater has migrated into the aquifer causing a considerable increase in the groundwater salinity.

Geophysical methods have been recognized as one of the most efficient techniques for the quantitative and qualitative assessment of groundwater resources.

Fig. 1 Location map of the study area including monitoring (*blue*) and production (*triangular*) wells and locations of 2D profiles (*red lines*)

Specifically, earth resistivity methods have a wide application on shallow groundwater resources. The application of surface resistivity methods to delineate the contaminated zones has the following advantages: (1) reduced need for intrusive techniques and direct sampling (2) relatively inexpensive and can be used for rapid and economical monitoring of large areas and optimization of the required number of monitoring wells; and (3) electrical conductivity/resistivity are intrinsic properties of ground-water chemistry that are readily interpreted in terms of the degree of groundwater contamination (Ebraheem et al. 1990; Ebraheem et al. 1997; and El Mahmoudi 1999).

The electrical conductivity of water, which is controlled by the concentration of dissolved ions, shows how well the groundwater conducts electricity. For example, fresh water in the Wadi Ham area has a chloride ion concentration of 224 ppm and a specific conductivity (SC) of 0.98 mS/cm. Saline water in Wadi Ham has chloride levels of 15,000–30,374 ppm and an SC of 20–79 mS/cm (Fig. 2). This 100-fold difference in SC can produce a similar difference in the conductivity of geologic materials saturated with fresh or saline water. Therefore, the use of 2D resistivity imaging method in the assessment of groundwater quality and identification of the dispersion zone in the coastal aquifers is justified.

This paper is concerned with the application of earth resistivity imaging methods along with water hydrogeochemistry to identify and classify the dispersion zone, where the groundwater salinity/resistivity varies gradually, in the coastal aquifer of Wadi Ham. By combining hydrogeological and geophysical data with hydrogeochemical data from monitoring wells, an empirical relationship between earth resistivity and total dissolved solids (TDS) was obtained. This empirical relationship was then used to identify the fresh, brackish, and saline-water zones.

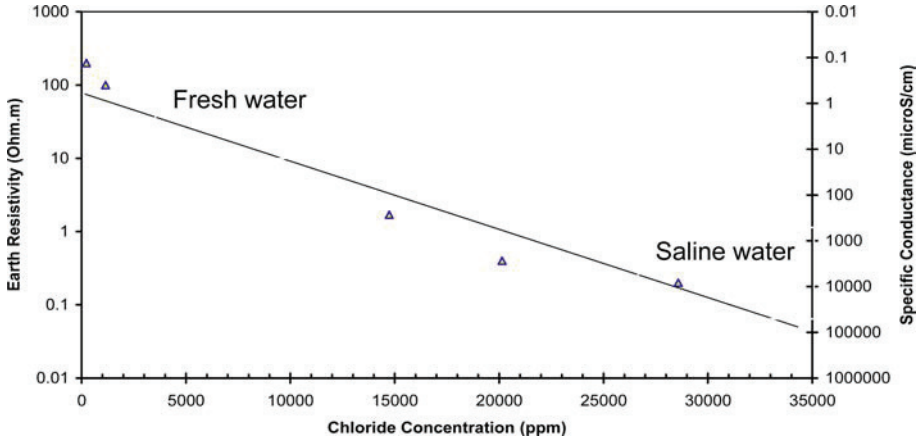

Fig. 2 The relationship between chloride concentration (ppm), earth resistivity (Ohmm), and water specific conductance (micro S/cm)

Geological and hydrogeological setting

The geological map of Wadi Ham area (Fig. 3) indicates that the upstream part of the area is dominated by the Masafi Mountains whereas the alluvial plains prevail in its lower part. Sediments of the lower plains are composed of recent Pleistocene wadi gravels. The alluvium gravels layer overlays the consolidated rocks of the Semail formation (Ophiolite sequence) with a separating mantle of fractured zones at some locations. The wadi gravels are poorly sorted and sub-rounded to sub-angular gravel. The degree of consolidation varies from recent uncemented sandy gravel to the older well cemented and consolidated gravels. Clastics size ranges from silt grade to boulder material with a very high sand content. The thickness of the unconsolidated material layer varies from 15 to 100 m along the profile running from Dam of Wadi Ham to the coast (Fig. 1). This dam was completed in 1989 to harvest the surface water runoff from rainfall events and recharge the groundwater. The minimum thickness of this layer is found in the area of well number BHF-19 which is upstream of the Wadi Ham dam close to the mountain series. The maximum thickness of the same layer is found in the area of well number BHF-14 which is very close to the coast of Oman Gulf. The unconsolidated material layer is composed of an upper sub-layer of gravels underlain by another layer of sand. In the upstream part of the area, the thickness of the gravel sub-layer increases on the expense of the sand sub-layer. Near the shoreline, the thickness of the sand sub-layer increases on the expense of the gravel sub-layer (Figs. 4–6).

The gabbros and serpentinite of the Semail Ophiolites lie beneath the unconsolidated material layer. The gabbros/diorite are likely to be confined in some places by the cemented units within the base of the overlying layer. The depth to the Ophiolites layer varies from 15 to 100 m. The basement Ophiolites layer is generally dipping towards the coast as well as towards the wadi course (Fig. 4).

Based on the interpretation of the available data, two aquifers can be identified, namely the Quaternary aquifer which constitutes the main aquifer and is composed of the unconsolidated sediments (mainly alluvium gravel and coarse sand) and the fractured Ophiolites aquifer.

Electrowatt (1981) subdivided sediments of the Quaternary aquifer into recent sediments, being slightly silty sand gravel with some cobbles and boulders, and old sediments, which are silty sandy gravels with many cobbles and boulders which are weathered and cemented. The hydraulic conductivity of the recent sediments tends to be very high, typically in the range of 6–17 m/day. For the old cemented sediments the hydraulic conductivity is in the range of 0.086–0.86 m/day. In the unconsolidated gravels the primary porosity is very high compared to the cemented gravels. The storage coefficients typically range from 0.1 to 0.3 (Electrowatt 1981). IWACO (1986) conducted 14 pumping tests (duration ranged from 8 to 300 min) on some of the wells located in the study area. The results of these pumping tests, in addition to the results of one pumping test conducted for well Ob1, Sherif et al. (2004), were interpreted using two different softwares.

The results are summarized in Table 1. Based on the obtained transmissivity values, the outlet area of Wadi Ham can be divided into two zones. The first zone is about 2 km wide and 3.5 km long and is extending directly downstream of the dam with a saturated aquifer thickness of 10–40 m. This zone has transmissivity values ranging from less than 100 to about 200 m^2/day. The second zone is the coastal plain which extends about 4.5 km in length and more than 8 km in width, with a saturated aquifer thickness ranging from 50 to 100 m. It has a transmissivity of more than 1,000 m^2/day. Figure 7 presents a contour map for the transmissivity in the area.

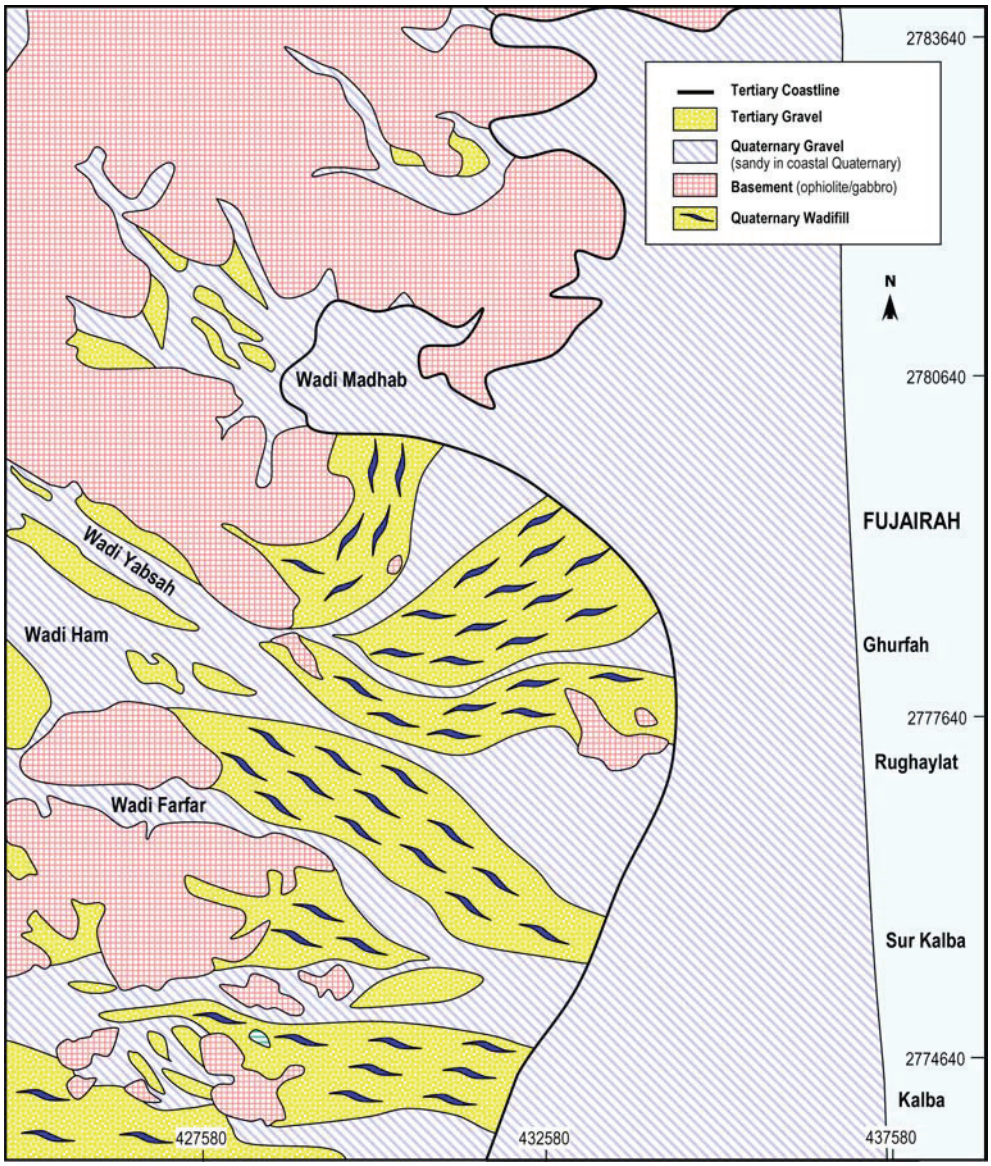

Fig. 3 Geological map of Wadi Ham area

Groundwater pumping and levels

Groundwater in Wadi Ham is exploited intensively from the sand and gravel aquifer for irrigation in the coastal plain between Fujairah and Khor Kalba. Several well fields are in operation for the domestic water supply by the Ministry of Electricity and Water including:

(a)Fujairah well field: The total pumping from this field used to be 3.2 million m^3/year until 1988, after which very limited groundwater is pumped.
(b)Shaara well field (located 2 km downstream of Wadi Ham and including 9 wells): They started in the year 1988 with a total extraction of 1.0 million m^3/year and a pumping duration of 10 hr/day. Out of 9 wells available, 5 wells dried up in the year 2003. Discharges of the wells were reduced significantly between 1988 and 2003.
(c)A new well field near Kalba: The field was operated since 1995 with a total pumping of 6.0 million m^3/year.To determine the impact of groundwater extraction and the effect of the constructed dam on the groundwater level, the Ministry of Agriculture and Fisheries has adopted a monthly monitoring program for groundwater levels. The monitoring network includes 16 observation wells located in Wadi Ham. Figure 8 presents the monthly rainfall plotted on the same graph with groundwater levels for the period 1987–2004. A significant variation in groundwater levels in response to

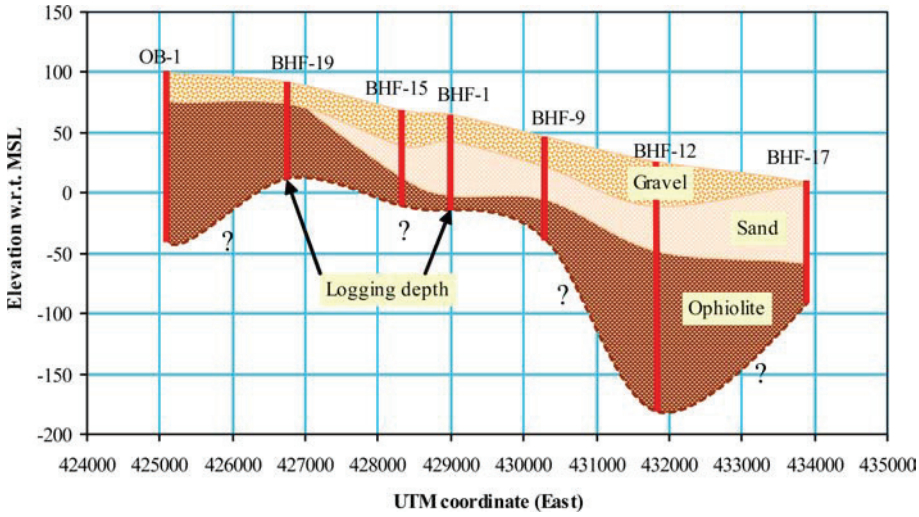

Fig. 4 A NW–SE subsurface geological cross-section along Wadi Ham course. The *bottom* of Ophiolite layer is not shown as the wells are only penetrating the upper zone of this very thick layer

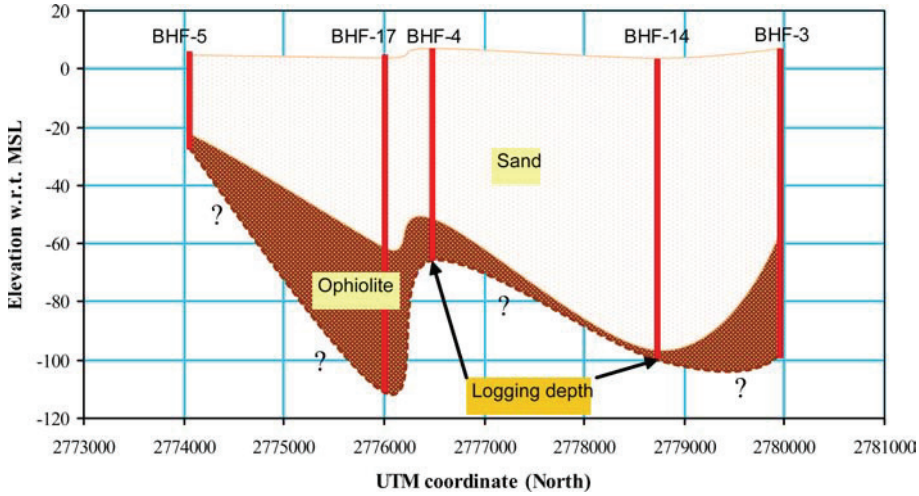

Fig. 5 A N–S subsurface geological cross-section across Wadi Ham near the shoreline. The *bottom* of Ophiolite layer is not shown as the wells are only penetrating the upper zone of this very thick layer

rainfall events and groundwater extraction is observed. The fluctuation of the groundwater levels varied between 2 and 40 m in the observation wells. In both wet and dry periods, the hydraulic gradient of groundwater in the plain area is very mild as compared to the gradient within the wadi valley close to the dam area. In general, groundwater levels in all observation wells are declining since 1996 (the last wet year). The lowest levels were encountered in the year 2004 indicating the current prevailing drought conditions. Wells that are located near the dam of Wadi Ham are much more sensitive to rainfall and recharge from the ponding area.

Hydrogeochemical parameters

To study the hydrogeochemical parameters of the groundwater in Wadi Ham, 35 water samples were collected in January 2004 from the existing production wells that are owned by the Federal Authority of Water and Electricity. These water samples were given the same identification numbers as the wells (Fig. 9). All of the sampled wells are tapping the Quaternary Alluvium Aquifer in the outlet area of Wadi Ham. The samples were chemically analyzed for major cations and anions and the results are listed in Table 2. The obtained results are discussed hereafter in term of the regional hydrogeochemical aspect and horizontal zonation of the groundwater.

Electrical conductivity (EC)

Measuring the electrical conductance of the groundwater provides a rapid determination on TDS. Specific electrical conductance defines the conductance of a cubic centimeter of water at a standard temperature of 25°C (Todd 1980). It is a function of water temperature, types

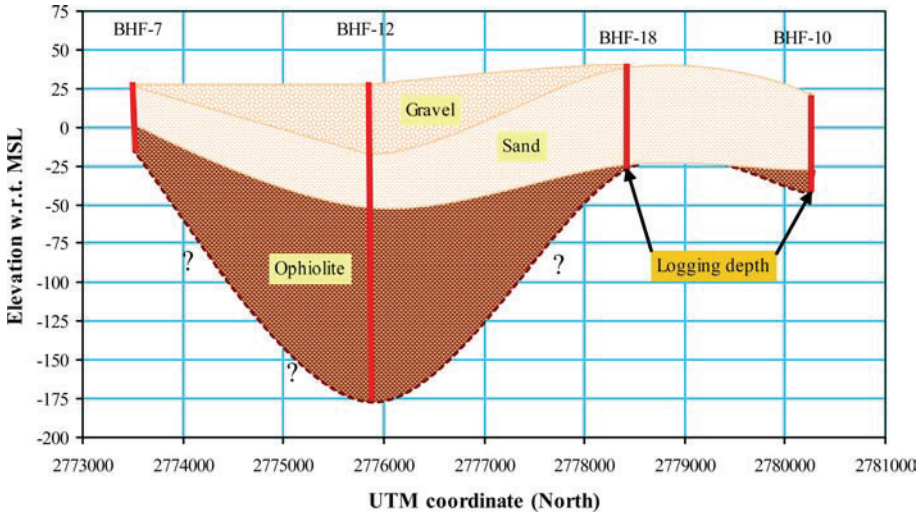

Fig. 6 A N–S subsurface geological cross-section across Wadi Ham, about 3 km from Oman Gulf. The *bottom* of Ophiolite layer is not shown as the wells are only penetrating the upper zone of this very thick layer

Table 1 Estimated aquifer parameters

Borehole	UTM coordinate Northing	T (IWACO, 1986) m^2/day Easting	Transmissivity m^2/day	Hydraulic conductivity m/day				Storativity
				Cooper and Jacob (1946)	Theis (1935)	Theis (1935)	Cooper and Jacob (1946)	
BHF-1	2,779,163	429,211	30	101	148	7.76	11.4	0.00161
BHF-3A	2,779,800	432,900	3,450	6,246	744	14	118	6.21×10^{-8}
BHF-4A	2,776,995	433,773	8,630	11,700	9,120	203	259	2.01×10^{-15}
BHF-5	2,773,400	432,950	4,347	8940	1,260	105	745	1.33×10^{-20}
BHF-10	2,780,250	431,800	1,230	480	258	6.79	12.6	0.00197
BHF-11	2,781,000	430,450	386	101	151	4.73	3.16	0.00666
BHF-12	2,776,432	431,865	1340	947	789	15.5	18.6	0.00239
BHF-13	2,774,900	427,800	8.5	4.13	3.83	25.6	27.5	0.0101
BHF-14	2,778,750	433,900	2,882	4,750	3,630	39.4	51.6	3.03×10^{-7}

of present ions and their concentrations. Therefore, all measurements of electrical conductivity were adjusted to a temperature of 25°C so that the variations in conductance will only reflect the variations in the concentration and types of the dissolved solids. The electrical conductance of the collected water samples varied between 1,750 and 81,900 μS/cm.

Total dissolved solids

The TDS in a water sample are a measure of all solid materials in solution whether ionized or not. It does not include suspended sediments, colloids or dissolved gases. The TDS content in groundwater is an indication of its salinity. Table 3 provides a simple classification for the groundwater type based on total concentration of dissolved constituents.

Groundwater in the study area varies from brackish water in the northwest and northeast parts of the study area to saline water in the remaining part. Groundwater salinity has a high value (> 20,000 ppm) in the central zone (Fig. 10). This high salinity is probably due to the intensive pumping activities in this specific area to meet irrigation and domestic water supplies of the cities of Fujairah and Kalba. The depression of the groundwater levels may have caused upcoming of the saline water as well.

Hydrogen ion concentration (pH)

The hydrogen ion concentration of groundwater is a measure of its acidity or alkalinity. The pH value of water is related to its quality and affects, to a great extent, its suitability for different uses. The pH is controlled by the amount of dissolved carbon dioxide (CO_2), carbonates (CO_3^{2-}) and bicarbonates (HCO_3^-) The hydrogen ion concentrations (pH) of the collected groundwater samples ranged between 6.13 and 7.87, which means that the groundwater in the study area ranges between slightly acidic- due to dissolving of the various gases in the atmosphere by rainwater and the decay of vegetable matter- to slightly alkaline caused mainly by carbonates (CO_3^{2-}) and bicarbonates (HCO_3^-) of cations.

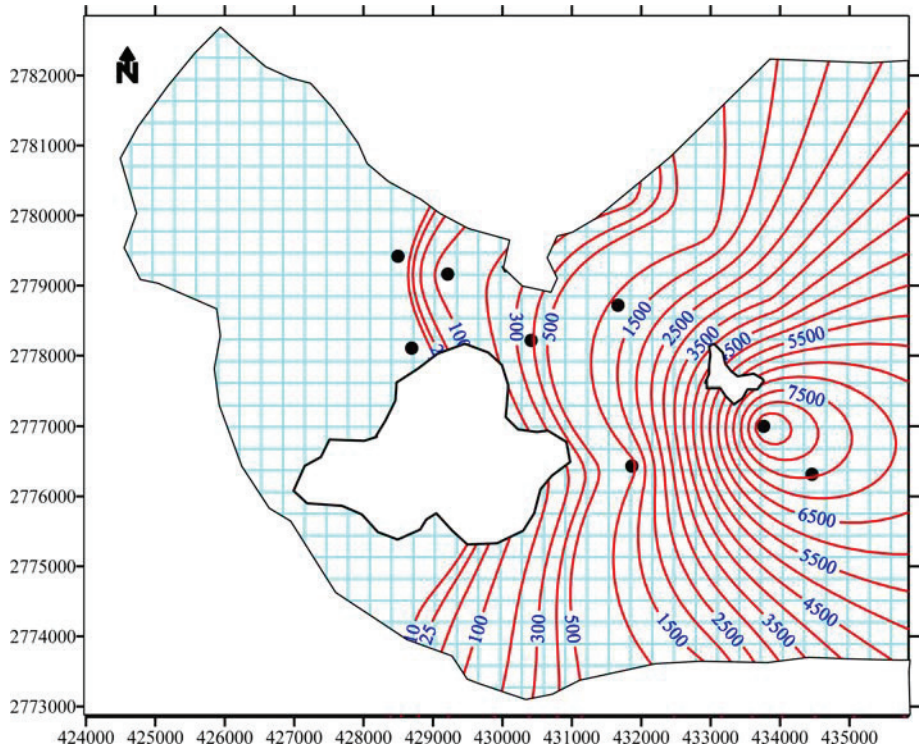

Fig. 7 Distribution of transmissivity (m^2/day) in the study area

Anions and cations

The results of the chemical analyses of the collected groundwater samples (Table 2) indicated the following sequence of anions and cations, respectively.

$$Cl^- > SO_4^{2-} > HCO_3^-,\ Cl^- > HCO_3^- > SO_4^{2-},$$
$$Mg^{2+} > Ca^{2+} > Na^+,\ Ca^{2+} > Mg^{2+} > Na^+,\ \cdot$$
$$Na^+ > Mg^{2+} > Ca^{2+},\ Na^+ > Ca^{2+} > Mg^{2+}$$

According to the hypothetical salt combination and

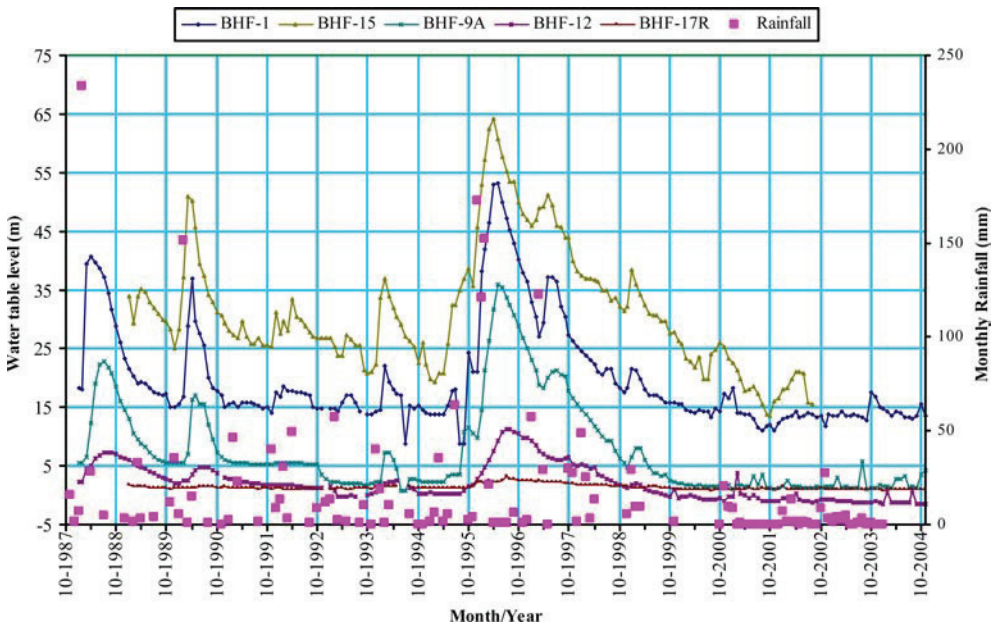

Fig. 8 Groundwater levels in observation wells and rainfall events, 87–2004

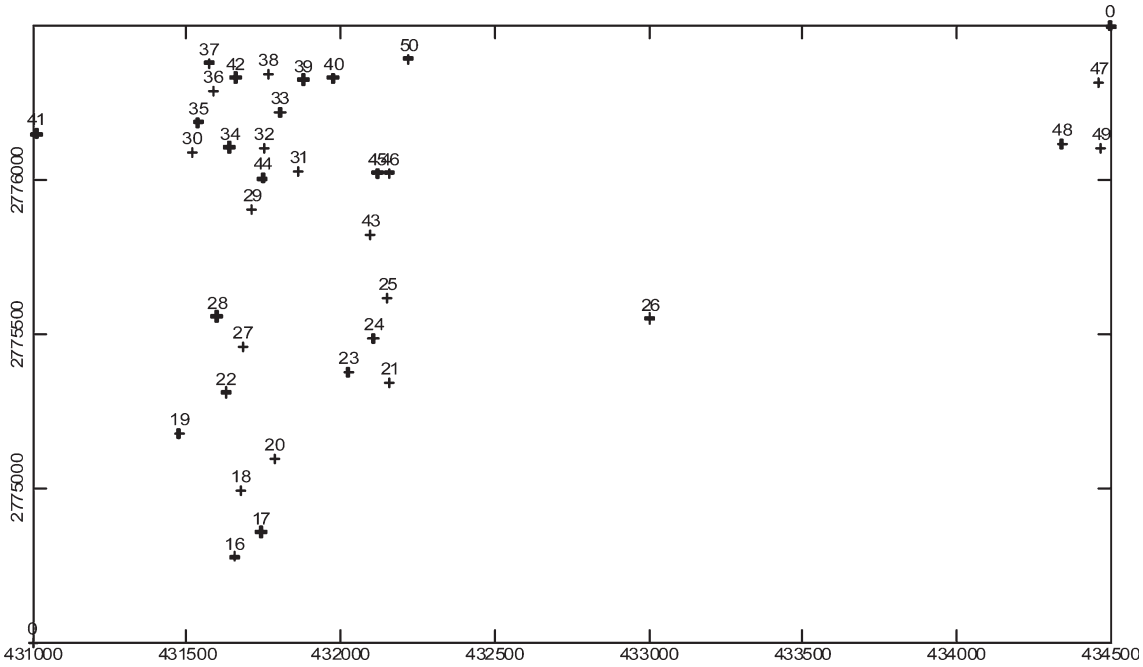

Fig. 9 Location map of collected groundwater samples in the wadi outlet area

sequence of anions and cations there are five different zones of groundwater in this study (Fig. 11). The compositions of the groundwater of the study area varied from north to south. The groundwater changes from HCO_3–chloride/Mg-calcium water type (in the north) to sodium chloride water type as TDS increases (in the south). This change can also be shown by Stiff's (1951) graphical method (Fig. 12). It can be deduced that the mixing of different water types in the middle part of the study area is severe which caused by salt water upcoming due to intensive groundwater abstraction.

Geoelectrical techniques: principles of DC resistivity method

DC resistivity methods measure the electrical resistivity distribution of the subsurface using current transmitted into the ground from dc- or low-frequency sources by two electrodes (A and B). The potential difference between a second pair of electrodes (M and N, Fig. 13), is also measured. The apparent resistivity of the subsurface can be calculated by applying a geometric correction (G) to Ohm's law ($R = \Delta V/I$, where R is the resistance, ΔV is the measured potential difference, and I is the injected current), based on the specific electrode spacing and geometry. These geometrically corrected measurements are defined as apparent resistivities rather than true resistivities because a homogeneous subsurface is assumed. Measured resistivity values are controlled by material resistivity, quality, and quantity of groundwater (Haeni et al. 1992; Sharma 1997; Reynolds 1997). The maximum penetration depth is directly proportional to the electrode spacing and inversely proportional to the subsurface conductivity (Edwards 1977, Mussett and Khan 2000).

2D dc-resistivity profiling is carried out by making many measurements at different locations along the profile and at different offsets. The 2D dc-resistivity profiling data are inverted to create a tomogram-like model of resistivity along a section of the subsurface that can be used to detect water zones of different salinities.

Due to the unavailability of a 2D dc-resistivity profiling system, a single channel Memory Earth Resistivity and IP Meter instrument manufactured by AGI Advanced Geosciences, Inc., was used with four wheels of electric wires as a substitute for the multicore cable and a manual reading instead of the control unit. The linear array of each profile consisted of 24 electrodes where the distances were controlled manually by marching through the profile forward and backward. Wenner array (Fig. 13a) was used in this survey. By using an iterative smoothness-constrained least-squares inversion method (deGroot-Hedlin and Constable 1990; Sasaki 1992), apparent resistivity data collected by the 2D dc-resistivity system are inverted to create a model of subsurface resistivity that approximates the true subsurface resistivity distribution (Loke 1997). In this study, four 2D dc-resistivity profiles were completed. The locations of these profiles were chosen based on the available monitoring wells for calibration purposes.

The geophysical and hydrogeological data were processed as follows. The SC measurements of well-water

Table 2 Hydrogeochemical parameters of analyzed groundwater samples, January 2004

No	Easting	Northing	Ca^{2+}	Mg^{2+}	Na^{+}	K^{+}	HCO_3^-	SO_4^-	Cl^-	KCl	NaCl	$MgCl_2$	$CaCl_2$	TDS (ppm)	EC (μS/cm)
16	431,654	2,774,777	1,080	1,416	966	17	366	643	6,923	0.2	20	55	25	11,411	21,750
17	431,741	2,774,859	1,960	1,524	1,219	21	488	1,082	8,804	0.2	19	45	35	15,098	27,850
18	431,675	2,774,994	2,120	1,404	1,265	23	500	978	8,875	0.2	20	42	38	15,165	28,950
19	431,474	2,775,176	2,080	1,428	1,242	21	512	726	9,017	0.2	20	43	38	15,026	28,350
20	431,785	2,775,096	1,620	1,560	5543	48	732	1,835	1,4307	0.3	53	28	18	25,645	45,700
21	432,158	2,775,343	1,560	1,596	6,256	55	976	1,603	15,443	0.3	56	27	16	27,489	48,500
22	431,628	2,775,311	1,580	1,572	5,060	44	793	1,733	13,561	0.3	51	30	18	24,343	43,300
23	432,024	2,775,377	1,540	1,620	5,014	48	854	1,882	13,419	0.3	51	31	18	24,377	43,400
24	432,106	2,775,486	1,840	1,404	6,417	61	732	2,040	15,446	0.3	57	24	19	27,940	49,150
25	432,151	2,775,618	1,800	1,428	6,233	59	763	1,921	15,230	0.3	56	24	19	27,434	48,350
26	433,004	2,775,551	1,500	1,548	5,980	52	793	1,792	14,733	0.3	56	27	16	26,398	46,900
27	431,681	2,775,459	1,700	1,452	5,014	55	702	2,059	13,171	0.3	51	28	20	24,153	42,450
28	431,597	2,775,558	1,360	1,164	5,336	44	1,055	1,382	12,496	0.3	58	24	17	22,837	40,900
29	431,711	2,775,905	1,840	1,164	3,381	25	610	1,183	10,721	0.2	44	29	27	18,924	34,000
30	431,517	2,776,090	336	156	973	20	476	231	2,130	0.7	58	18	23	4,322	7,590
31	431,863	2,776,028	1,640	1,596	5,083	48	1,190	1,618	13,632	0.3	51	30	19	24,807	44,000
32	431,751	2,776,103	1,600	1,560	4,945	47	671	1,690	13,490	0.3	51	30	19	24,003	43,200
33	431,803	2,776,222	1,440	1,536	5,934	57	1,037	1,411	14,662	0.3	56	28	16	26,077	46,050
34	431,638	2,776,107	1,480	1,056	3,174	24	580	1,877	8,946	0.2	46	29	25	17,137	29,800
35	431,536	2,776,189	90	61	186	4	256	27	463	0.6	46	27	0	1,087	1,750
36	431,585	2,776,288	94	62	185	5	244	32	476	0.7	45	28	26	1,098	1,800
37	431,571	2,776,381	96	65	201	6	250	38	504	0.8	46	28	0	1,160	1,910
38	431,765	2,776,343	760	1,008	2,254	22	336	1,056	6852	0.3	45	38	17	12,288	22,000
39	431,878	2,776,328	1,380	1,140	5,451	46	1,019	1,363	12,674	0.3	59	23	17	23,073	40,900
40	431,975	2,776,333	1,480	1,584	6,049	51	903	2,088	14,626	0.3	56	28	16	26,781	47,050
41	431,012	2,776,150	2,040	1,692	7,912	75	1,171	2,626	18,283	0.3	59	24	17	33,799	59,550
42	431,658	2,776,335	200	222	570	21	299	188	1,598	1	46	34	19	3,098	5,460
43	432,096	2,775,821	1,520	996	6,210	46	988	1,627	13,490	0.3	63	19	18	24,877	43,700
44	431,747	2,776,006	1,820	1,140	3,910	28	744	1,224	11,325	0.2	48	26	26	20,191	35,900
45	432,119	2,776,024	1,610	1,524	5,382	42	1,086	1,089	1,4271	0.2	53	28	18	25,004	44,200
46	432,159	2,776,024	1,760	1,656	7,590	153	1,464	2,203	17,395	0.7	59	24	16	32,221	55,950
47	434,462	2,776,316	2,100	972	16,146	421	915	3,782	28,578	1.2	78	9	10	52,914	81,900
48	434,342	2,776,120	1,360	1,128	4,370	37	811	1,469	10,970	0.3	54	26	19	20,145	35,700
49	434,469	2,776,106	1,640	1,380	5,520	5	1,049	1,306	13,987	0	55	26	19	24,887	44,150
50	432,221	2,776,395	1,460	1,104	1,426	18	427	1,075	7,029	0.2	27	40	32	12,539	23,050

samples were converted into water resistivities ($\rho_w = 1/\sigma_w$). To ensure that the observed values of earth resistivity are representative of the saturated zone, the earth resistivity, ρ_e, was measured at Wenner a-spacing approximately seven times the depth to the water table. These data (Table 4) have been used to obtain an empirical relationship between earth resistivity and water resistivity, and subsequently between earth resistivity and TDS. The procedure described by Cartwright and Sherman (1972), Cartwright and McComas (1968), Ebraheem et al. (1990), and El Mahmoudi (1999) was used to obtain these empirical relationships.

Table 3 Types of groundwater based on TDS contents in mg/l (Fetter 2001)

Water type	TDS (mg/l)
Fresh water	0–1,000
Brackish water	1,000–10,000
Saline water	10,000–100,000
Brine	>100,000
Water type	TDS (mg/l)
Fresh water	0–1,000
Brackish water	1,000–10,000
Saline water	10,000–100,000
Brine	>100,000

Correlation between earth resistivity and groundwater quality

Hydrogeochemical and geophysical data were evaluated and interpreted to study the relationship between earth resistivity and hydrochemical properties of the groundwater. Based on this relation, the transition (dispersion) zone between the fresh water body and the seawater body in the coastal area of Wadi Ham can be identified.

Many researchers (e.g. Cartwright and Sherman 1972, Ebraheem et al. 1990, and Ebraheem et al. 1997) reported the possibility to identify a correlation between earth resistivity and the amount of TDS in groundwater. In this study the TDS is computed as the sum of the following major ionic components: Ca^{2+}, Mg^{2+}, total Fe, Na^{+},

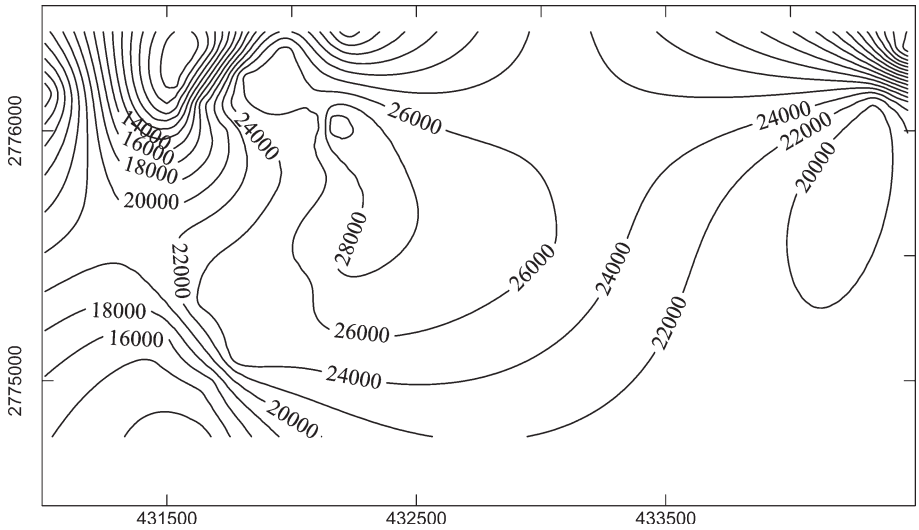

Fig. 10 Isosalinity (in ppm) contour map of the outlet area of Wadi Ham

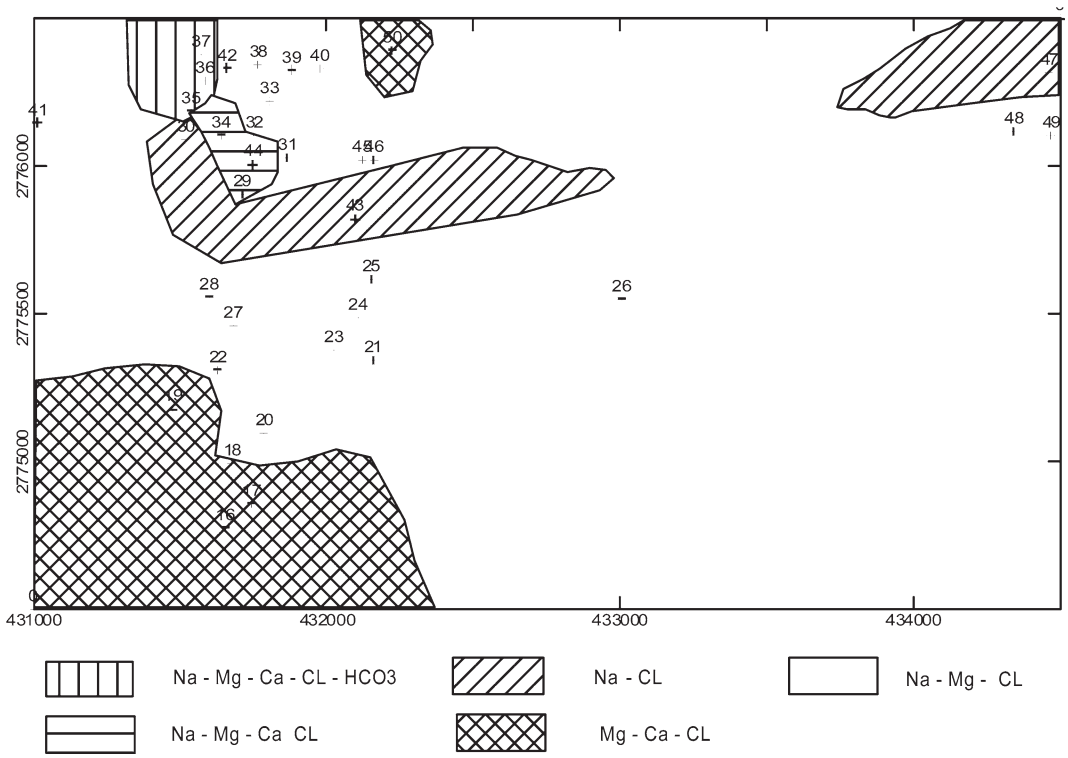

Fig. 11 Hydrogeochemical zonation map of the outlet area

K^+, HCO_3^-, SO_4^{2-}, Cl^-, and NO_3^-. These ions comprise 90% of the TDS in natural water (Freeze and Cherry 1979).

The water resistivity was plotted as a function of earth resistivity. The best-fit straight line between earth resistivity (ρ_e) and water resistivity (ρ_w) indicates the following empirical relationship (Fig. 14):

$$\rho_e = 19.206\rho_w$$

where ρ_w is the water resistivity, and ρ_e is the earth resistivity in Ohmmeters.

The obtained good fit between earth resistivity and water resistivity ($R^2 = 0.995$) reveals that the earth resistivity in the outlet area of Wadi Ham (where the Quaternary aquifer is composed of gravels and coarse sand and the water table is very shallow) is strongly

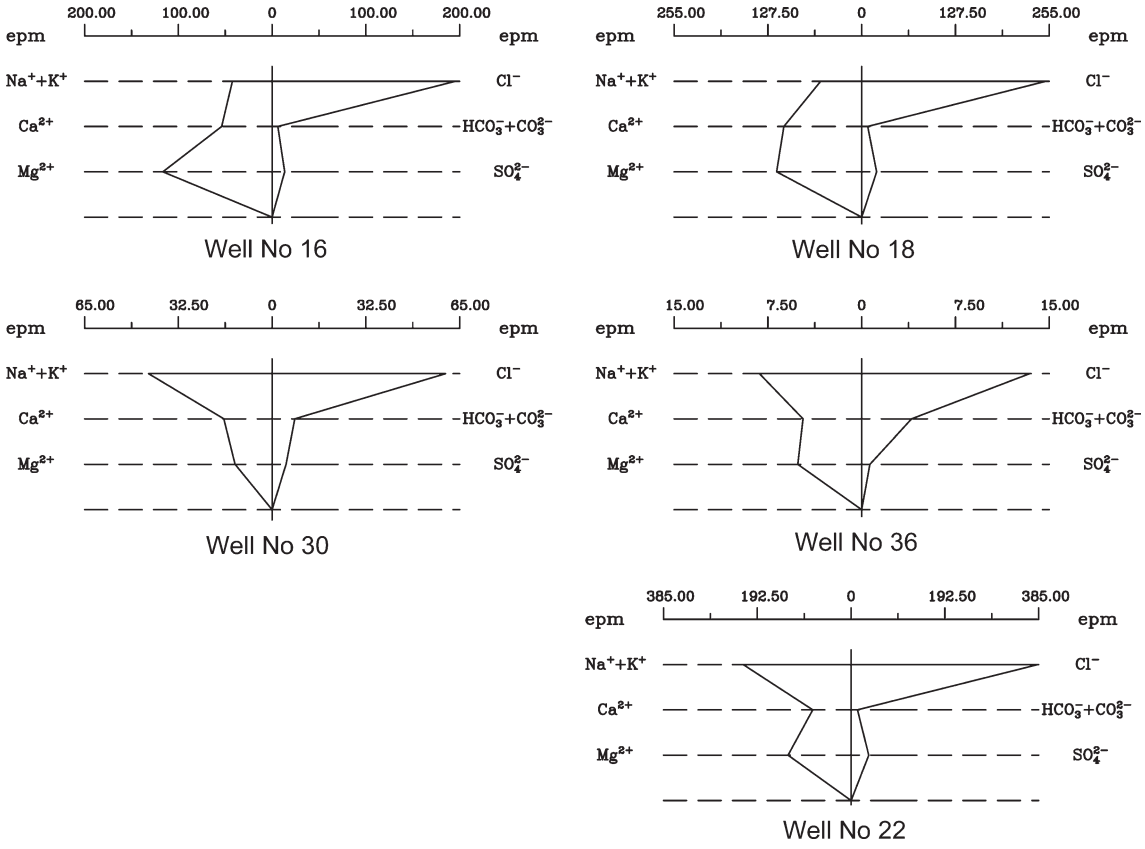

Fig. 12 Stiff diagram for the different groundwater types

affected by groundwater salinity. This observation provides a reaffirmation of the basis for applying resistivity methods to study the salinity distribution in groundwater.

Earth resistivities and TDS were also plotted, as shown in Fig. 15, and the fitted line indicates the following empirical relationship:

$$\text{Log TDS} = 4.403 - 0.7343 \text{Log}\,\rho_e$$

where, TDS is the TDS in parts per million. This relation reveals that three different types of groundwater may be delineated. These types are fresh ($\rho_e > 30\ \Omega$ m), brackish ($1 < \rho_e < 30\ \Omega$ m), and saline groundwater ($\rho_e < 1\ \Omega$ m). It is also possible to plot water SC, σ_w (in μ mho/cm), versus TDS, as presented in Fig. 16. The fitted line reveals the following empirical relationship:

$$\text{TDS(ppm)} = 0.6906 \rho_w (\mu \text{mho/cm}).$$

Freshwater/seawater interface

The 2D apparent resistivity data were inverted to create a model of the resistivity of the subsurface using Res2dinv software. Res2dinv uses an iterative smoothness-constrained least-squares method (deGroot-Hedlin and Constable 1990; Sasaki 1992).

To test interpretation, resistivity models were created based on the inversion results. The resistivity models were used to generate synthetic apparent resistivity data. The synthetic apparent resistivity data were inverted using Res2dinv and the resulting inversions were compared with the original inverted resistivity section. The resistivity models were adjusted and simplified to qualitatively match the field-data inversions. Generating resistivity models helped to constrain interpretation of the field-data inversions and to identify locations and orientations of resistivity anomalies. Then the variations of TDS concentration with depth were estimated by applying the above empirical relationships on the inverted 2D resistivity data and constrained by the salinity measurements of water samples from nearby existing water wells.

The 2D dc-resistivity field-data inversions, resistivity models and synthetic-data inversions for profile 1 (near the shoreline and BHF-17, Fig. 1) are shown in Fig. 17. Figure 18 presents a fence diagram of the true resistivity in the four studied profiles. In profile 1, the depth of penetration, which is approximately 50 m, did not reach the top surface of the Ophiolites bedrock. The cross section of

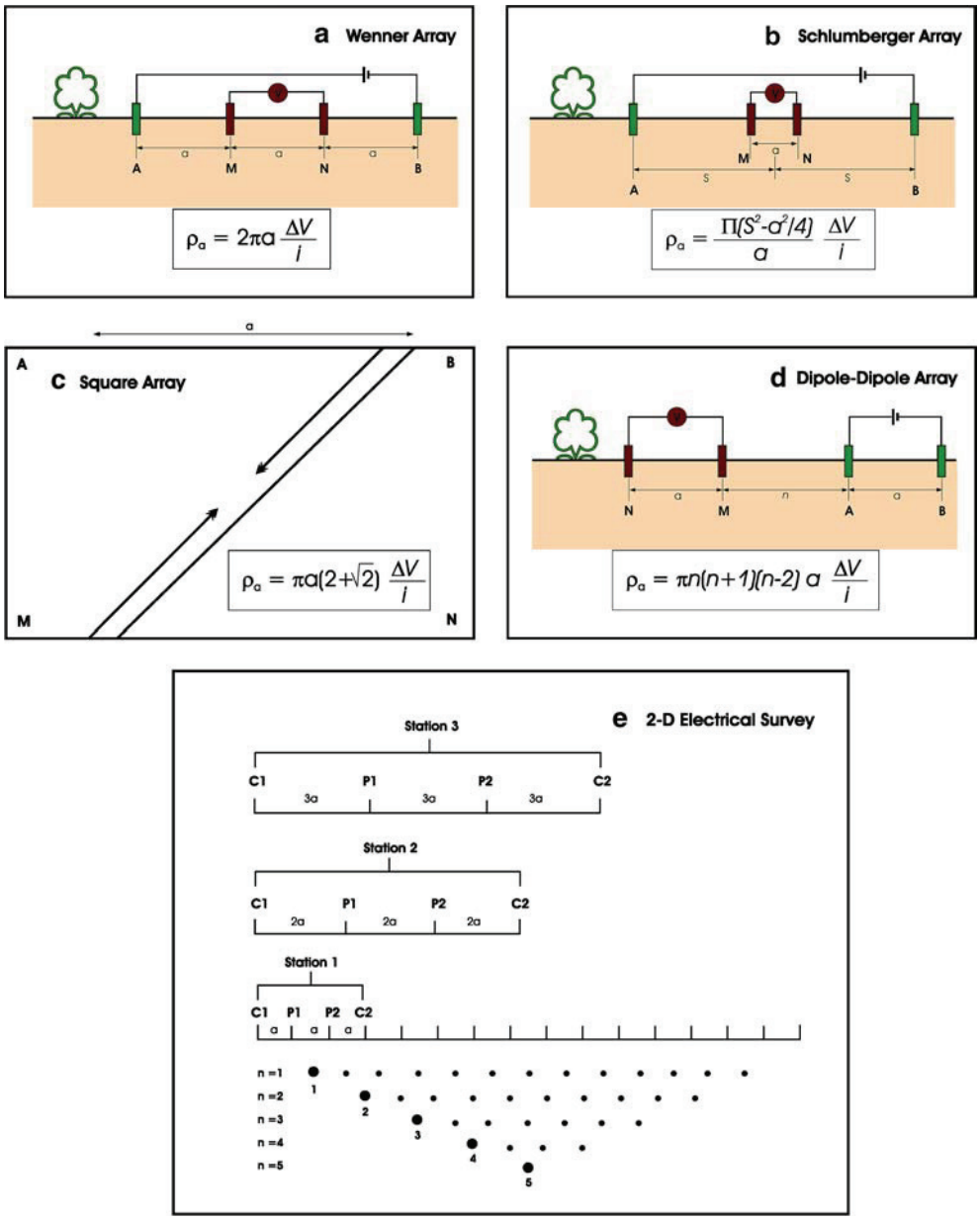

Fig. 13 DC resistivity setting, **a**–**d** common electrode arrays used in DC resistivity and their corresponding geometric factors, and **e** arrangement of electrodes for a 2D electrical survey and the sequence of measurements

Table 4 Geophysical and hydrogeological data used for obtaining the empirical relationship

Well no.	Water table depth (m)	Water conductance (μmho/cm)	Soil conductance (μmho/cm)	Water resistivity (Ohmm)	Earth resistivity (Ohmm)	Measured TDS (ppm)	Chloride concentration (ppm)
BHF-17	7.6	81,900	50,000	0.1221	0.2	55,692	28,578
BHF-4	13.22	60,840	20,000	0.164366	0.5	43,583	20,142
F-23	16	46,900	5,882	0.21322	1.7	31,892	14,733
BHF-12	28.5	1,690	100	5.91716	100	451	1,149
BHF-15	35	980	50	10.20408	200	627	224

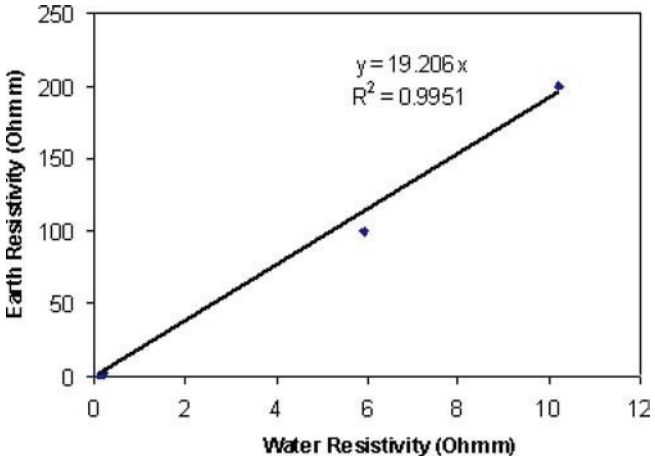

Fig. 14 Empirical relationship between water and earth resistivities (Ohmm)

the true resistivity beneath profile 1 represents the variation in the lithology and degree of saturation of the alluvium gravel layer as well as groundwater quality. The depth to water table (the layer colored in light blue in the depth-true resistivity section shown in Fig. 17) is ranging from 11 to 15 m below ground surface. Its true resistivity is ranging from 30 to 70 Ωm and it is ranging in thickness from less than a meter in the center of the profile (near agricultural farms) to only few meters at the sides of the profile. The brackish and saline water zone is very thick below this profile and marked with a resistivity range of 1–30 Ωm. Only in the central area the saline zone which has true resistivity values of less than 1 Ωm is observed (dark blue). It is worth to mention that, the 1 Ωm refers approximately to electric conductance value of 10,000 μS/cm (or TDS of 6,400 ppm approximately).

Profile 2 (Fig. 18b), is located 800 m to the west of profile 1 and is parallel to it. The inversion results of this profile data indicate that the thickness of fresh zone started to increase, particularly in the northern part near Fujairah Airport. At the same time the thickness of the brackish water zone decreases. The saline water zone can only be seen in the southern side near Kalba town (dark blue in Fig. 18b with a resistivity range of less 1 Ωm).

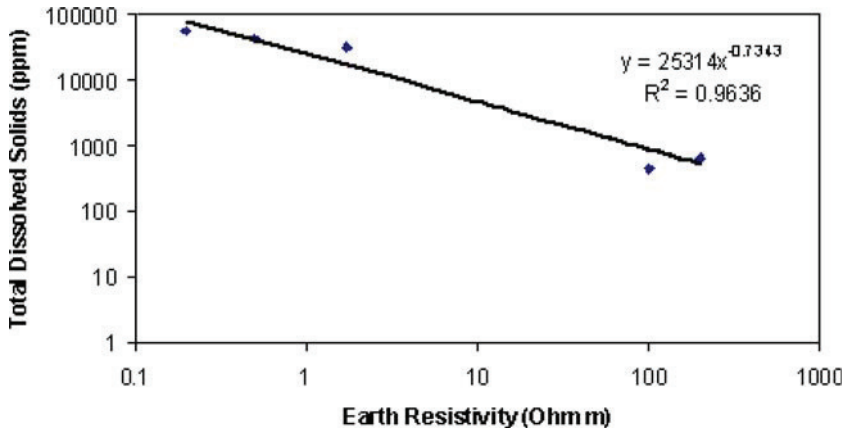

Fig. 15 Empirical relationship between TDS (ppm) and earth resistivity (Ohmm)

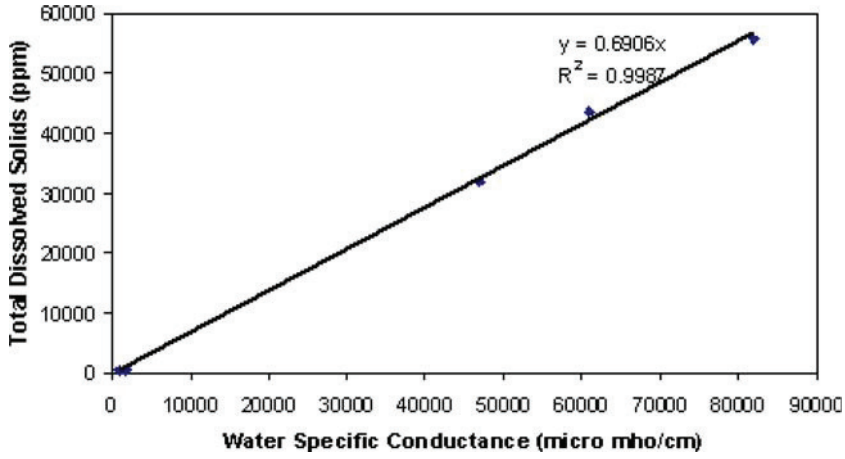

Fig. 16 Empirical relationship between TDS (ppm) and water specific electrical conductivity (μ mho/cm)

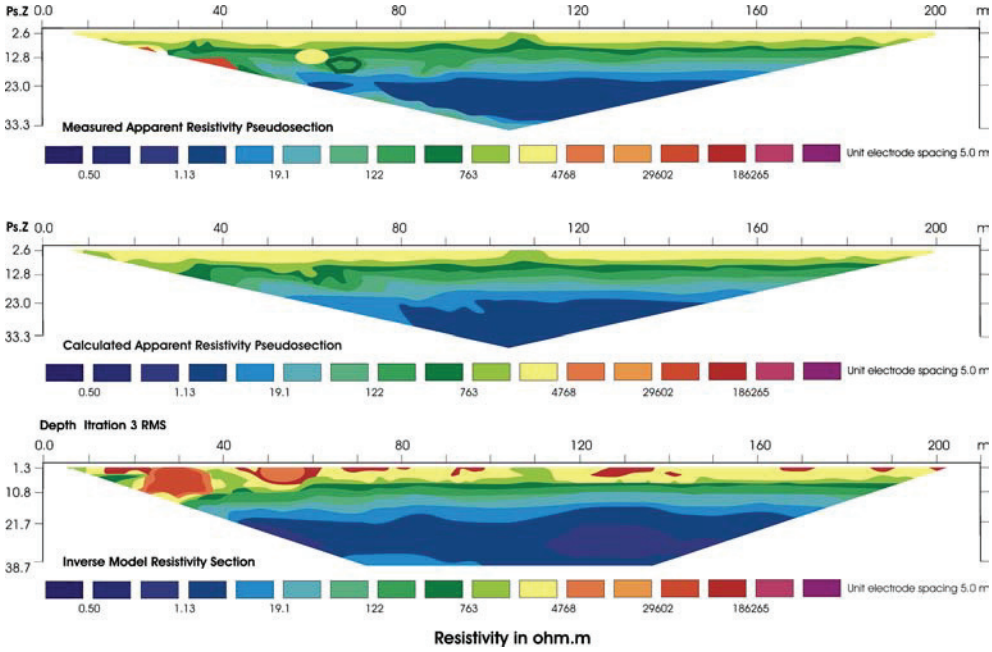

Fig. 17 Inverted resistivity section for two-dimensional direct-current data for profile Ham-1

Profile 3, Fig. 18c, is located 800 m to the west of profile 2 and parallel to it. The interpretation results of this profile indicate that along the total length and to its maximum depth of penetration which is about 40 m the fresh and brackish water zones are encountered. The thickness of the freshwater zone has increased. However, the upcoming of brackish water due to the depression in groundwater levels caused by intensive irrigation in the middle part of the area is remarkable.

Profile 4, Fig. 18d, is located 800 m to the west of profile 3 and is parallel to it. Along the total length of this profile and to its maximum depth of penetration the freshwater zone is observed. The thickness of the freshwater zone is much bigger than in profiles 1, 2 and 3.

Figure 18 indicates that the salinity of groundwater due to seawater intrusion increases mainly eastward toward the shore line and to a lesser extent southward which probably caused by excessive irrigation in Kalba area or due to its bay which is around 10 km away from the study area.

Conclusions

Two aquifers can be identified in the area of Wadi Ham, the Quaternary aquifer and the fractured Ophiolites aquifer. The Quaternary aquifer is regarded as the main aquifer and is composed of the unconsolidated sediments (mainly alluvium gravel and coarse sand). The sediments of the Quaternary aquifer are highly permeable and tend to be unconsolidated near the ground surface, becoming better cemented and consolidated with depth.

The Quaternary aquifer is directly recharged from the percolating rainfall. Historical groundwater measurements indicate a significant variation in the response to recharge events and groundwater abstractions from one area to the other. Wells located in the vicinity of the ponding area of Wadi Ham are more sensitive to precipitation and recharge events. Since 1996 (the last wet year), groundwater levels in all observation wells have been declining. The quality of the groundwater in the study area varies from brackish water in the northwest and northeast parts of the area to saline water in the remaining parts.

Empirical relationships have been obtained between water resistivity, earth resistivity and TDS. The relationship between earth resistivity and TDS, together with inverted 2D true resistivity-depth sections can be used to identify the average TDS at any point and at any depth along the 2D resistivity profiles. Therefore, it was possible to classify the groundwater as fresh, brackish, or saline. Thickness of the freshwater zone is varying from less than 1 m near the shoreline to about 20 m at distance 3 km from the shore line. Earth resistivity methods represent feasible and efficient tools for quantitative and qualitative studies related to groundwater resources in coastal aquifers.

Excessive groundwater exploitation may seriously affect the groundwater quality through the phenomenon of saline upcoming. Therefore, it is important to maintain the balance between the fresh and saline water bodies in the coastal aquifer of Wadi Ham.

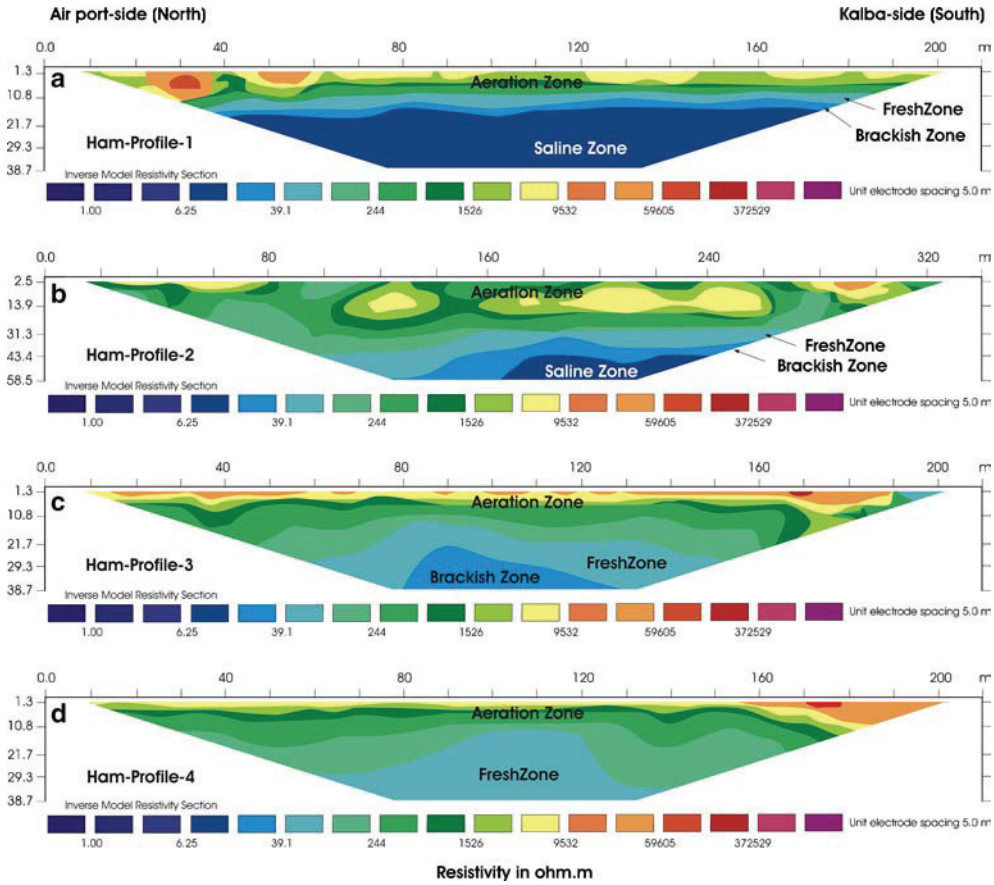

Fig. 18 Combined diagrams of the four true resistivity sections of Wadi Ham showing the increase of seawater eastward

Acknowledgements This study was funded by the joint United Arab Emirates University — Sultan Qaboos University collaboration research project (no. 01/7/60/2003). The help and support of the Ministry of Agriculture and Fisheries, Dubai, and Sharjah Electricity and Water Authority, UAE to complete the field activities are highly appreciated. We would also like to thank Prof. Dr. Sigrid Dörhöfer, Editor and anonymous reviewer of Environmental Geology Journal for their valuable comments

References

Cartwright K, McComas MR (1968) Geophysical surveys in the vicinity of sanitary landfills in northeastern Illinois. Ground Water 5:23–30

Cartwright K, Sherman F (1972) Electrical earth resistivity surveying in landfill investigations. 10th Annual Engineering and Soils Engineering Symposium, Moscow, ID

Cooper HH, Jacob CE (1946) A generalized graphical method for evaluating formation constants and summarizing well field history. T Am Geophys Un 27:526–534

deGroot-Hedlin C, Constable S (1990) Occam's inversion to generate smooth, two-dimensional models from magnetotelluric data. Geophysics 55(12):1613–1624

Ebraheem AM, Hamburger M W, Bayless ER, Krothe NC (1990) A study of acid mine drainage using earth resistivity measurements. Ground Water 28(3):361–368

Ebraheem AM, Senosy MM, Dahab KA (1997) Geoelectrical and hydrogeochemical studies for delineating groundwater contamination due to saltwater intrusion in the northern part of the Nile Delta, Egypt. Ground Water 35(2):216–222

Edwards LS (1977) A modified pseudosection for resistivity and IP. Geophysics 42(5):1020–1036

Electrowatt E. (1981) Wadi Bih dam and Groundwater recharge facilities. Internal Report: Vol. 1: Design, Ministry of Agriculture and Fisheries, Dubai, UAE
EL-Mahmoudi AS (1999) Geoelectric Resistivity Investigations of Kafr Saqr Sheet, Sharrqiya Governorate, East Nile Delta. J Petrol Min Eng 2(1):84–108
Fetter CW (2001) Applied Hydrogeology,4th edn. Prentice Hall Inc., New Jersey, p 598
Freeze AR, Cherry JA (1979) Groundwater. Prentice Hall Inc., New Jersey
Haeni FP, Placzek, Gary, Trent RE (1992) Use of ground-penetrating radar to investigate infilled scour holes at bridge foundations. In: Hanninen, Pauli and Autio, Sini (eds) Fourth International Conference on Ground Penetrating Radar, Rovaniemi, Finland, June 8–13, 1992, Proceedings: Geological Survey of Finland Special Paper 16, p. 285–292
IWACO (1986) Groundwater Study Project 21/81, Drilling of deep water wells at various locations in the UAE. Groundwater Development in the Northern Agricultural Region. Internal Report (vol. 7), Ministry of Agriculture and Fisheries, Dubai, UAE
Loke MH (1997) Electrical imaging surveys for environmental and engineering studies–a practical guide to 2D and 3D surveys: Penang, Malaysia, University Sains Malaysia, unpublished short training course lecture notes
Mussett AE, Khan MA (2000). Looking into the Earth: An Introduction to Geological Geophysics. Cambridge University Press, p 492
Reynolds JM (1997) An introduction to applied and environmental geophysics. Wiley, New York, p 796
Sasaki Y (1992) Resolution of resistivity tomography inferred from numerical simulation. Geophys Prospect 40:453–464
Sharma PV (1997) Environmental and engineering geophysics. Cambridge University Press
Sherif M et al (2004) Assessment of the Effectiveness of Al Bih, Al Tawiyean and Ham Dams in Groundwater Recharge using Numerical Models, Interim Report. Ministry of Agricultural and Fisheries, Dubai, UAE
Stiff HA (1951) The interpretation of chemical water analysis by means of patterns. J Petrol Technol 3:15–17
Theis CV (1935) The realation between the lowering of the piezometric surface and the rate and uration of discharge of a well using groundwater storage. T Am Geophys Un 2:519–524
Todd DK (1980) Groundwater hydrology, 2nd edn. Wiley, New York, p 535